Ionics
https://doi.org/10.1007/s11581-025-06536-2

RESEARCH

Mg^{++} ion conducting polyethylene oxide/magnesium triflate quasi-solid state electrolyte for rechargeable Mg^{++} battery application

H. N. M. Sarangika[1] · M. A. K. L. Dissanayake[2,3] · G. K. R. Senadeera[2,4]

Received: 26 April 2025 / Revised: 16 June 2025 / Accepted: 5 July 2025

Abstract

In this study, we demonstrate the potential of a gel polymer electrolyte based on polyethylene oxide (PEO), complexed with magnesium triflate [$Mg(CF_3SO_3)_2$] and plasticized with ethylene carbonate (EC) and propylene carbonate (PC), for use in rechargeable magnesium batteries. The optimized composition, PEO (12.20 wt%), $Mg(CF_3SO_3)_2$ (14.6 wt%), EC (36.6 wt%), and PC (36.6 wt%) achieves a notable ionic conductivity of 2.52×10^{-3} S cm^{-1} at room temperature, which increases with temperature according to Arrhenius behavior. The electrolyte demonstrates a high Mg^{2+} ion transference number ($t_{Mg}{}^{++} = 0.51$) and a high total ionic transference number ($t_{\text{ion}} = 0.98$) highlighting its excellent performance as an Mg^{2+} ion conductor. Preliminary battery tests with the cell configuration Mg/PEO:EC:PC:$Mg(CF_3SO_3)_2$/TiO_2-C show a discharge capacity of 65 mA h g^{-1} at a 0.015C rate, with an open-circuit voltage of 1.85 V. These results suggest that the PEO:EC:PC:$Mg(CF_3SO_3)_2$ gel polymer electrolyte is a promising candidate for application in magnesium-based electrochemical devices.

Keywords Mg^{++} ion conductor · Gel polymer electrolyte · TiO_2 cathode · Mg^{++} ion battery

Introduction

The world is facing an impending energy crisis due to the depletion of non-renewable energy sources including coal, oil, and natural gas, which is causing global energy consumption to rise. These fossil fuels are limited and being used at an unsustainable rate, despite having fuelled industrial progress and development for more than a century. In addition to endangering their long-term availability, their extraction and usage accelerate climate change by releasing greenhouse gases into the atmosphere and causing air pollution. There is a pressing need to switch to more sustainable energy systems as fossil fuel sources are depleting and the environmental effects of using them worsen. While renewable energy sources such as wind, solar, and hydropower are viable options, there is still work to be done in developing and widely implementing clean, efficient technologies. In order to ensure a sustainable energy future, this energy crisis emphasizes the need for creative solutions, such as developments in energy storage, energy efficiency, and alternative clean fuels. As the supply of traditional energy sources decreases, the world faces serious threats to its economy, society, and environment if it does not transition to renewable resources.

Because they make it possible to store and use renewable energy sources more effectively, rechargeable batteries are essential to solving the energy dilemma. Rechargeable batteries offer an alternative by storing extra energy produced during periods of peak production and making it available during times of high demand or low output of renewable energy.

Lithium-ion (Li-ion) batteries have become the dominant energy storage technology in modern devices and systems due to their high energy density, long cycle life, and relatively lightweight design. Originally developed in the 1970s and commercialized by Sony in the 1990s, Li-ion batteries have revolutionized energy storage by powering a wide range of technologies from portable electronics to electric

✉ H. N. M. Sarangika
sarangikah@appsc.sab.ac.lk

[1] Department of Physical Sciences and Technology, Faculty of Applied Sciences, Sabaragamuwa University of Sri Lanka, Belihul Oya 70140, Sri Lanka

[2] National Institute of Fundamental Studies, Hantana Road, Kandy 20000, Sri Lanka

[3] Postgraduate Institute of Science, University of Peradeniya, Peradeniya 20400, Sri Lanka

[4] Department of Physics, The Open University of Sri Lanka, Nawala, Nugegoda 11222, Sri Lanka

Published online: 14 August 2025

vehicles (EVs) and large-scale renewable energy storage systems.

Li-ion batteries play a major role particularly in the areas of communication, computers, and portable electronic devices and also in high power storage devices such as batteries in hybrid and all electric vehicles. Thus, science and technology of rechargeable Li ion batteries dominates the current R&D activities, and research is being continued worldwide on the development of high power and high energy density secondary Li ion batteries, mainly driven by the demand for hybrid and all electric vehicles. Despite their numerous advantages, lithium-ion batteries are more expensive to manufacture than other forms of rechargeable batteries. Thermal runaway is a phenomenon in which a Li-ion battery overheats and may catch fire if damaged or badly handled. This has raised safety concerns, especially in large-scale applications such as EVs and grid storage. While Li-ion batteries have a long cycle life, they do degrade with time, with capacity steadily decreasing after multiple charge and discharge cycles. This is a concern for long-term uses [1, 2]. Another major concern is the limited availability of lithium metal in the earth's crust, thereby making the cost of lithium batteries to go up rapidly in the near future. Relative abundance of Mg, Ti, and Li metals in earth's crust is Mg: 29,000 ppm, Ti: 6600 ppm, and Li: 17 ppm [3–7].

Magnesium-ion (Mg-ion) batteries have developed as a possible alternative to lithium-ion (Li-ion) batteries in response to growing demand for more sustainable, safer, and high-performance energy storage solutions [8]. Mg-ion batteries have various potential advantages over Li-ion technology, making them a viable alternative for future energy storage solutions. Magnesium is the eighth most prevalent element in the Earth's crust, making it significantly more readily available and less expensive to obtain than lithium. Magnesium is a divalent ion, which means it can carry two positive charges (Mg^{2+}) per ion, compared to lithium, which is monovalent (Li^{+}) and carries only one charge per ion. This gives Mg-ion batteries the potential to store more energy in the same volume compared to Li-ion batteries. Magnesium's abundance offers a more sustainable and scalable option for battery production, lowering concerns over resource depletion and lowering costs. Theoretically, the multivalent nature of magnesium permits a higher energy density, which may result in batteries with longer lifespans and more capacity for power storage. Compared to lithium metal, which has a specific capacity of 3860 mAh/g and a volumetric capacity of 2061 mAh/cm^3, magnesium metal offers a specific capacity of 2205 mAh/g and a significantly higher volumetric capacity of 3833 mAh/cm^3 [9, 10]. This means that energy-dense battery technologies based on magnesium metal may perform better than lithium-based systems, especially in applications that call for large-scale energy storage or high-capacity portable devices [11]. Mg^{++}ion battery was first demonstrated by Aurbach et al. in the year 2000 [12] and after that the development of a Mg battery technology has received much attention as a potential rechargeable battery.

A typical Mg battery consists of three major components, the Mg anode, the cathode and a Mg^{++} ion conducting electrolyte. Performance of the battery largely depends on the active material, cathode. Hence, selecting a cathode material is a critical issue to develop a Mg battery with high energy and power density. Recent research on magnesium-ion batteries has concentrated on producing cathode materials that can successfully host magnesium ions (Mg^{2+}).

When discharging a Mg battery, dissolution of Mg^{++} ions from the negative electrode (anode) and their intercalation into positive electrode (cathode) takes place. During the charging intercalated Mg^{++}ions are released from the positive electrode (cathode) and Mg^0 deposition in the anode takes place. Numerous intercalation materials such as metallic oxides, metallic sulfides, selenides, and polyanion compounds have been tested as possible cathode materials for Mg^{++} ion rechargeable battery [13–19]. According to reported data, in most cases, the insertion of Mg proceeds in the same potential region as the insertion of Li in Li^+ ion batteries [20]. Metal oxides are considered to be the most promising cathode materials for high energy density secondary Mg batteries due to their higher working potentials and better chemical, electrochemical, and thermal stabilities. High degree of ionic character of the metal oxygen bond in these oxides generally leads to higher oxidizing power of the compound and produces a high voltage battery. However in most Mg batteries, V_2O_5-based materials [14, 15] are used as the cathode material because of the limited cycling stability of other metal oxides. These cathode materials are expensive and rare. Therefore, the use of these materials limits their practical applications. TiO_2, on the other hand, is a low cost, highly abundant, nontoxic, and environmental friendly material. Hence, exploring the possibility of using TiO_2 as a cathode material in rechargeable battery technology is important. TiO_2 has been already explored as alternative negative electrode for the rechargeable Li batteries due to its higher theoretical storage capacity of 335 mA h g^{-1} [21, 22]. However, practical specific capacity of TiO_2 is less than that of their theoretical capacity due to two main limitations. Poor electronic conductivity and low Li^+/Mg^{++} diffusivity in the TiO_2 could directly affect the possibility of achieving a higher practical specific capacity [10]. Nano-structured TiO_2 with their large surface area, however, paves the way for its wide utilization as electrode for rechargeable batteries. The loosely packed nano-particles expose more area to the electrolyte solution, and this may cause to improve the diffusion of electrolyte solution through the nano-structured TiO_2. Although extensive research has been undertaken on TiO_2-based Li^+/Mg^{++} hybrid batteries, only a few studies have documented TiO_2 as a cathode material in Mg ion

batteries. F-doped TiO_2 nano crystals produced by hydrothermal method recently demonstrated a 77.2 mA h g^{-1} capacity as a cathode material in magnesium ion batteries with $[Mg_2Cl_3]+[AlPh_2Cl_2]-$/THF electrolyte [23]. A magnesium battery using a magnesium borohydride/tetraglyme electrolyte, a titanium dioxide cathode, and a magnesium anode demonstrated a discharge capacity of 155.8 mA h g^{-1}[24]. In this work, for the first time, we report a Mg ion battery composed of a Mg anode, a TiO_2 cathode, and PEO. EC:PC:$Mg(CF_3SO_3)_2$ electrolyte.

Another constraint for developing a rechargeable magnesium battery is finding suitable Mg^{++} ion conducting electrolytes [25]. The possibility of internal shorting, leaks, and producing combustible reaction products at the electrode surface are the major problems associated with liquid electrolytes. By using a thin film of solid polymer electrolyte (SPE) or a gel polymer electrolyte (GPE) instead of conventional liquid electrolytes, several advantages can be gained. To be employed in a solid state or quasi-solid state battery, SPE or GPE film must have numerous features, including excellent ionic conductivity and mechanical stability.

Polyethylene oxide (PEO)–based SPEs possess good mechanical strength and dimensional stability, but its conductivity at ambient temperature is rather low, and it is in the order of 1×1^{-8} S cm^{-1}. In order to achieve high ionic conductivity, while retaining the mechanical properties, quasi-solid or gel polymer electrolytes (GPE) are investigated at present. Although the mechanical strength of a GPE is less than that of SPE, its ionic conductivity is in the adequate range (typically, 1×10^{-4} S cm^{-1}–1×10^{-3} S cm^{-1}) for battery applications [25]. PEO complexes with magnesium salts have moderate ionic conductivity (ranging from 10^{-5} to 10^{-4} S cm^{-1}) at temperatures about 80–100 °C, according to numerous investigations. Here, we present a few examples of PEO-based electrolytes utilized in Mg ion batteries. PEO-$Mg(CH_3COO)_2$-EC-PC [26] electrolyte exhibited 6.1×10^{-5} S cm^{-1} ionic conductivity. The room temperature ionic conductivity of the PEO-1-ethyl-3-methylimidazolium trifluoromethanesulfonate (EMITf)-magnesium trifluoromethanesulfonate $(MgTf)_2$ electrolyte [27] combination was 5.6×10^{-4} S cm^{-1}. A magnesium (Mg)-ion-conducting polymer electrolyte made of poly(ethylene oxide) (PEO) and Mg trifluoromethanesulfonate (Mg triflate or $Mg(Tf)_2$) with varying proportions of nonionic polymeric crystal succinonitrile (SN) [28] demonstrated 6×10^{-4} S cm^{-1} ionic conductivity. Furthermore, our team reported on the complexation of (PEO) with magnesium triflate ($Mg(Tf)_2$ or $Mg(CF_3SO_3)_2$) and the incorporation of the ionic liquid (IL) (1-butyl-1-methylpyrrolidinium bis(trifluoromethanesulfonyl)imide (PYR14TFSI)) as an electrolyte for magnesium ion batteries. At room temperature, these batteries exhibit an ionic conductivity of 3.66×10^{-4} S cm^{-1} [29]. Ionic conductivity was measured as 1.795×10^{-5} S cm^{-1} in the TiO_2 nano-filler integrated $Mg(BH4)_2$:polyethylene oxide (PEO):propylene carbonate (PC) polymer gel electrolyte [30]. The Mg^{2+} ion transference number is a critical electrochemical parameter that represents the proportion of total ionic current carried by magnesium ions in an electrolyte. A high transference number is desirable for Mg batteries, as it indicates dominant Mg^{2+} conduction, enhancing efficiency and minimizing concentration polarization. Electrolytes based on $Mg(CF_3SO_3)_2$ exhibit relatively high Mg^{2+} transference properties, making them suitable for use in rechargeable battery applications [31, 32]. In comparison to earlier reported results, the electrolyte including PEO (12.20 wt%), $(CF_3SO_3)_2$ Mg (14.6 wt%), EC (36.6 wt%), and PC (36.6 wt%) in this study shows outstanding ionic conductivity and Mg^{++} transference number.

Therefore, in this work, we have studied the possibilities of using low cost TiO_2 as the cathode martial in magnesium ion batteries comprising a quasi-solid polymeric electrolyte based on polyethylene oxide (PEO) as the host matrix. The polymer electrolyte based on PEO complexed with Mg $(CF_3SO_3)_2$, in ethylene carbonate (EC), propylene carbonate (PC) co-solvent has been characterized using AC impedance spectroscopy, cyclic voltammetry (CV), and DC polarization measurements. The batteries with cell configuration Mg/PEO:EC:PC:$Mg(CF_3SO_3)_2$/TiO_2-C were fabricated, varying the amount of carbon until the cells exhibited the highest battery parameters such as the open circuit voltage and the short circuit current density.

Experimental

Materials

Polyethylene oxide (PEO, Mw = 400000) and magnesium trifluoromethanesulfonate ($Mg(CF_3SO_3)_2$) (abbreviated as magnesium triflate, MgTf) purchased from Sigma Aldrich; propylene carbonate (PC) and ethylene carbonate (EC) with purity > 98% purchased from Fluka; and fluorine-doped SnO_2-layered (FTO) glass (sheet resistance 12 Ω/sq) and TiO_2 (Degussa P-25) purchased from Solaronix SA were used as staring materials.

Electrolyte preparation

The electrolyte for the Mg battery was prepared by impregnating it into a porous separator using the following procedure. 0.12 g of magnesium trifluoromethanesulfonate ($Mg(CF_3SO_3)_2$) was dispersed in 0.3 g of propylene carbonate (PC), 0.3 g of ethylene carbonate (EC), and the mixture was stirred for few minutes for complete dissolution. Then, 0.1 g of polyethylene oxide was added to this solution and

the mixture was heated up to 80 °C under continuous stirring until a homogeneous viscous gel is formed. This viscous gel, hereafter called the gel polymer electrolyte (GPE) was then allowed to cool down to room temperature.

Conductivity measurements

The ionic conductivity of electrolyte samples was determined using impedance analysis by a computer controlled Metrohm Autolab (PGSTAT 128 N) impedance analyzer in the frequency range between 0.1 Hz and 10 MHz. For impedance measurements, a disc-shaped gel polymer electrolyte sample was sandwiched between two polished stainless steel (SS) electrodes with the configuration SS/GPE/SS. The sample assembly was placed in a furnace with a temperature controller, and impedance measurements were taken from room temperature up to 65 °C at 5 °C intervals. Conductivity values at each temperature were determined from the impedance measurements.

DC polarization measurements

The electronic contribution to the total ionic conductivity was estimated by the DC polarization measurements. In this method, DC polarization current was monitored as a function of time for the electrolyte sample sandwiched between two stainless steel blocking electrodes with the configuration SS/GPE/SS and by applying a 1 V DC across the sample.

The total ionic transference number (t_{ion}) of the polymer electrolyte was estimated by Wagner's method using the Eq. (1),

$$t_{ion} = \frac{I_i - I_f}{I_i} \quad (1)$$

where I_i is the initial current and I_f is the final steady state current.

In order to determine the Mg^{++} ion contribution to the total ionic conductivity a combination of AC and DC measurements were taken. Equation (2) was used to calculate the magnesium ion (Mg^{++}) transference number (t_{Mg+2});

$$t_{Mg+2} = \frac{I_s(\triangle V - r_0 I_0)}{I_0(\triangle V - r_s I_s)} \quad (2)$$

where I_0 and I_s are the initial and final steady state currents and r_0 and r_s are the cell resistance before and after applying the polarization voltage respectively. For finding the r_0 value, the electrolyte was sandwiched between two non-blocking Mg electrodes with the cell configuration Mg/GPE/Mg, and the complex impedance response of the symmetrical cell assembly was measured. Then, a small voltage pulse ($\triangle V = 0.3$ V) was applied to the cell until the polarization current reached a steady state after which the complex impedance was again measured [27, 33].

Cyclic voltammogram

Cyclic voltammogram of the symmetrical cells SS/GPE/SS and SS/Mg/GPE/Mg/SS were recorded using a computer controlled Metrohm Autolab potentiostat/galvanostat (PGSTAT 128 N) at 5 mV s^{-1} and 1 mV s^{-1} scan rates. The experiments were carried out at 30 °C.

Mg/GPE/TiO_2-C/FTO cell

A powder mixture (0.2 g) of 89wt% TiO_2, (0.025 g) of 11 wt% carbon powders, one drop of Triton-X (as a binder) and few drops of acetic acid were thoroughly ground with ethanol. This mixture was used to prepare the cathode pellets with 5-mm diameter and thicknesses 12 μm on fluorine-doped tin oxide (FTO) glass substrate and then sintered at 450 °C for 45 min. Since we need to minimize the amount of binder used in the cathode, we followed this unconventional method to prepare the TiO_2 cathode on different current collector (FTO). Sintering up to 450 °C completely removes the binder (Triton-X) used in preparing the cathode, and this will help to decrease the amount of binder used in preparing cathode as well as internal resistance of the battery and hence increase the battery capacity. It is impossible to remove binder by sintering with the use of other commonly used current collectors such as Cu and Al. The weight of the prepared TiO_2 electrode was in the 1–2 mg range out of which the weight of the active TiO_2 material was 89%. Thin, circular discs of magnesium metal were sectioned out of a Mg sheet, polished and cleaned using acetone. The weight of the magnesium pellet used as the anode was about 0.15 g.

The Mg/PEO:EC:PC:$Mg(CF_3SO_3)_2$/TiO_2-C cell (for brevity, hereafter referred to as SS/Mg/GPE/TiO_2-C/SS cell) was assembled in the air tight spring loaded cell holder using the anode, electrolyte and the cathode. Charge/discharge cycling characteristics of the cells were recorded at room temperature using the Metrohm Autolab (PGSTAT 128 N) potentiosat/galvanostat system.

Results and discussion

Characterization of the gel polymer electrolyte

Impedance analysis

The impedance spectra of the gel polymer electrolyte taken with the symmetrical cell with configuration, SS/GPE/SS exhibits a typical Nyquist plot consisting of a part of a large semicircle (not shown). Electrical response of the cell can

be explained on the basis of an equivalent circuit with a resistance of the SS/GPE interface (R_b) and a resistance of the GPE sample (R_s). This R_s value as determined from the intercept of the straight line with the real axis of the Z'' vs. Z' Nyquist plot is around 122 Ω which is similar to the R_s value obtained from the equivalent circuit.

The ionic conductivity of the gel electrolyte was calculated using the Eq. (3).

$$\sigma = l/R_s A \tag{3}$$

where l is the thickness of the electrolyte sample, A is the contact area between the electrolyte and the electrode, and the R_s is the measured resistance. Room temperature ionic conductivity is found to be 2.52×10^{-3} S cm^{-1} which is comparable with that of the PEO gel polymeric electrolytes based on Li salts. An Li^+ conducting electrolyte with 1.71×10^{-3} S cm^{-1} ionic conductivity that contained EC: PC (3:1) plasticizers was reported by Semnani et al. [34]. Munichandraiah et al. found that the presence of plasticizers increased ionic conductivity from 1×10^{-8} S cm^{-1} to around 1×10^{-5} S cm^{-1} at ambient temperature [35].

When preparing the electrolyte, EC and PC were used as the plasticizers to enhance the conductivity. These plasticizers decrease the viscosity of the polymer and facilitate the ionic transport by increasing the ionic mobility. High dielectric constant of EC will weaken the columbic forces between the cations and anions and promote ionic dissociation and increase the number of free ions and hence the ionic conductivity [34].

During impedance measurements the temperature of the samples was varied from 25 to 65 °C, and the measurements were taken at 5 °C intervals. The conductivity values were extracted from complex impedance plots. Figure 1a shows the conductivity (on log scale) variation with reciprocal of the absolute temperature. The linear shape of the graph suggests that the temperature dependence of the conductivity obeys the classical Arrhenius relation expressed by Eq. (4).

$$\sigma = \sigma_o exp(-E_a/RT) \tag{4}$$

where σ is the ionic conductivity, σ_o is the pre-exponential factor, E_a is the activation energy, R is the gas constant, and T is the temperature. Corresponding Nyquist plot at different temperature and the equivalent circuit is shown in Fig. 1b.

In order to confirm the Mg^{++} ion conduction in PEO:EC:PC:Mgtf system, impedance spectroscopy, CV, and transport number measurements are performed. Figure 2 shows the comparative impedance plots for the symmetrical cells consisting of PEO:EC:PC:Mgtf gel electrolyte with blocking (SS) and non-blocking (Mg) electrodes. Steep rising impedance pattern of SS/GPE/SS symmetrical cell indicates the ion blocking nature of SS-electrodes to the Mg^{++} ions at the electrode electrolyte interfaces. Semicircular

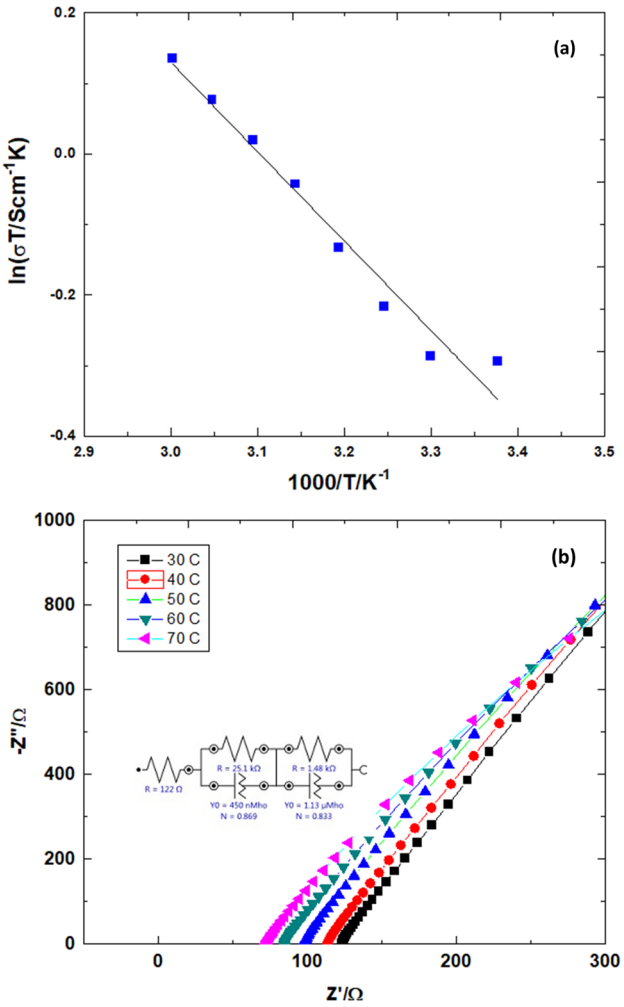

Fig. 1 **a** Temperature dependence of the ionic conductivity of the gel polymer electrolyte in logarithm scale. **b** Nyquist plot of gel electrolyte at different temperature and the equivalent circuit

dispersion curve obtained for the Mg/GPE/Mg shows the reversible nature of the Mg-electrodes in the polymer electrolyte. Further, the equivalent circuit well fitted with the Nyquist plot has high charge transfer resistance of the order of kΩ for the blocking interface while the cell, Mg/GPE/Mg shows small charge transfer resistance of the order of Ω associated with the redox process.

DC polarization results

The ionic transference number was estimated from DC polarization measurements to check the transference number of mobile species in the gel electrolyte (GPE) with composition PEO (12.20 wt%), $(CF_3SO_3)_2$ Mg (14.6 wt%), EC (36.6 wt%), and PC (36.6 wt%). Results of the DC polarization current measured as a function of time on application of DC potential of 1.0 V across the cell with

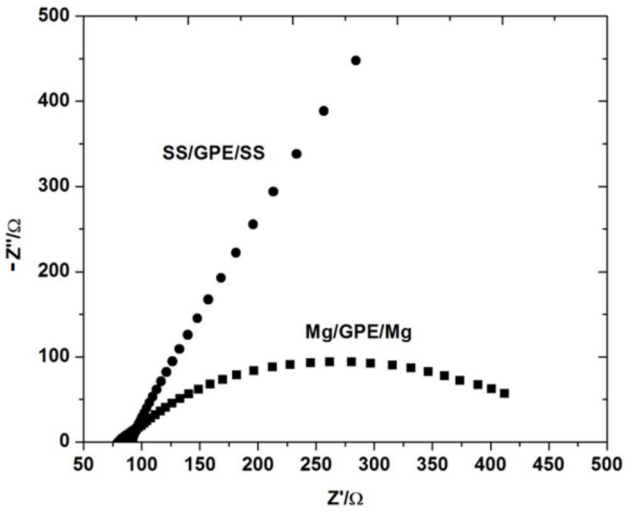

Fig. 2 Complex impedance plots for cell 1: SS/PEO:EC:PC:$Mg(CF_3SO_3)_2$/SS and cell 2: Mg/PEO:EC:PC:$Mg(CF_3SO_3)_2$/Mg recorded at room temperature

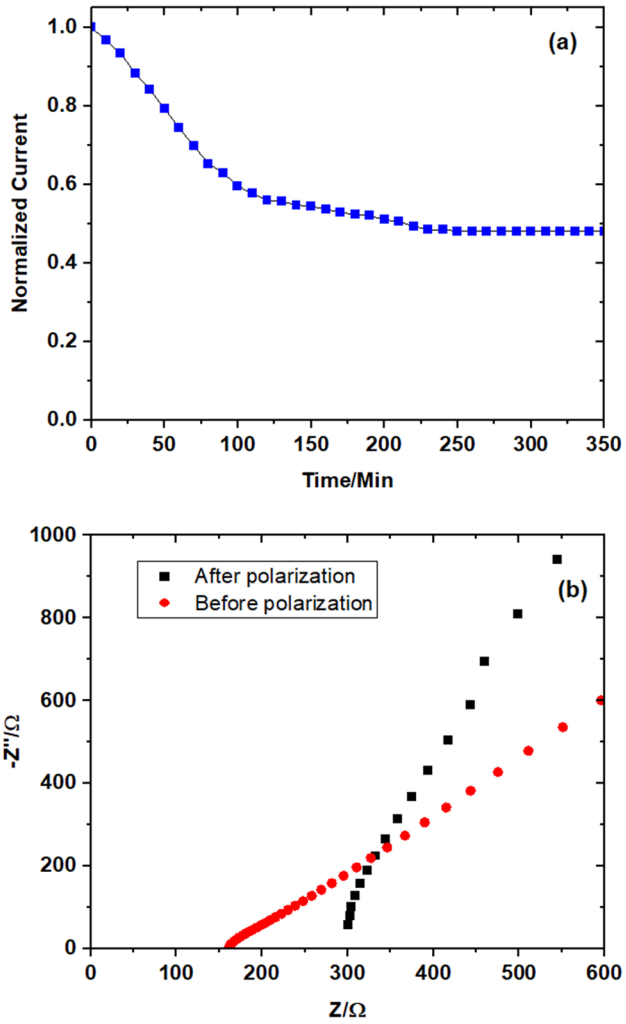

Fig. 3 **a** Variation of the dc polarization current (normalized) as a function of time for the Mg/GPE/Mg cell. **b** Complex impedance response of the Mg/PEO:MgTf:EC:PC/Mg cell measured before and after dc polarization

stainless steel (SS) blocking electrodes in configuration SS/GPE/SS show that the polarization current dropped by more than 98% from the initial value during the first 10 min and then gradually became steady after about 3 h. The total ionic transference number, t_{ion} estimated using the Eq. (1), is 0.985. This shows that the material is predominantly an ionic conductor, with Mg^{++} and $CF_3SO_3^{2-}$ as the dominant mobile ionic species. The total ionic conductivity of the electrolyte is made up of individual ionic conductivity contributions from Mg^{++} and $(CF_3SO_3)^{2-}$ ions. Mg^{++} ion contribution for the total ionic conductivity is important for the Mg battery, because Mg^{++}ions intercalate/de-intercalate into/from TiO_2 cathode during the charging/discharging cycles.

In order to determine the Mg^{++} ion transference number, Eq. (2) in the "DC polarization measurements" section was used. For this, AC impedance of the Mg/GPE/Mg symmetrical cell with the electrolyte sample of composition of PEO (12.20 wt%), $(CF_3SO_3)_2$ Mg (14.6 wt%), EC (36.6 wt%), and PC (36.6 wt%) was measured and the value of the resistance, R_o was determined. Subsequently, a DC polarization voltage of $\triangle V = 0.30$ V was applied across the symmetrical cell Mg/GPE/Mg and the initial current, I_o and resulting steady state current I_s after 3 h was recorded. Figure 3 shows the variation of DC polarization current as a function of time. The values of I_o and I_s determined from Fig. 3 (before normalization) are 2.17 μA and 1.11 μA respectively.

According to the DC polarization measurements, the resistance of the symmetrical cell has increased from an initial value (r_o) of 1.62×10^2 Ω to the final value (r_s) of 3.15×10^2 Ω. The Mg^{++} ion transference number, calculated according to Eq. (2) using the I_o, I_s, r_o, r_s, and $\triangle V$ values is 0.51. This shows that the Mg^{++} ion contribution to the total ionic conductivity is significant.

Similar to the widely accepted view of Li^+ ion coordination with ether oxygen in PEO:LiX electrolytes, in the PEO based Mg^{++} ion containing gel polymer electrolyte also, the Mg^{++} cations are expected to coordinate with the ether oxygen atoms in the polymer chain while the interaction of anions with the polymer is supposed to be weaker. The transport of the anions takes place by ionic diffusion through the electrolyte [36].

For the polyethylene oxide-lithium triflate $[(PEO)_8LiCF_3SO_3)]$ polymer-salt complex, the value of the cation diffusion coefficient varies between 0.34 and 0.41 in the temperature range 428 to 448 K. This means that both anions and cations contribute to the total ionic conductivity of the PEO based Li^+ gel electrolyte. It is also reported that

Table 1 Ionic conductivity and Mg ion transference number of PEO-based electrolytes

Polymer used/solvent	Mg salt	Conductivity/S cm^{-1}	Transference number	Reference
PEO/EC-PC	$Mg(CF_3SO_3)_2$	2.52×10^{-3}	0.51	This Paper
PEO/EC-PC	$Mg(CF_3SO_3)_2$	1×10^{-5}	-	[35]
PEO/EC-PC	$Mg(CH_3COO)_2$	6.1×10^{-5}	-	[26]
PEO/PC	$Mg(BH_4)_2$	1.795×10^{-5}	0.22	[30]
PEO/(EMITf)[a]	$Mg(CF_3SO_3)_2$	5.6×10^{-4}	0.45	[27]
PEO/(PYR14TFSI)[b]	$Mg(CF_3SO_3)_2$	3.66×10^{-4}	0.40	[29]
PEO/PVP[c]/methanol	$Mg(NO_3)_2$	5.8×10^{-4}	0.33	[37]
PEO/PMA[d]/DMC[e]/EC	$Mg[(CF_3SO_2)_2N]_2$	2.8×10^{-3}	-	[38]
PEO/PMA[d]/(EMITFSI)[f]	$Mg[(CF_3SO_2)_2N]_2$	10^{-4}	-	[39]

[a]1-ethyl-3-methylimidazolium trifluoromethanesulfonate

[b]1-butyl-1-methylpyrrolidinium bis(trifluoromethanesulfonyl)imide

[c]Poly(vinyl pyrrolidone)

[d]Poly(methacrylate)

[e]Dimethyl carbonate

[f]1-ethyl-3-methylimidazolium bis(trifluoromethylsulfonyl)imide

for the same electrolyte, the addition of PC reduces the cationic transference number by 46%. In the present study also, where magnesium trifluoromethanesulfonate (magnesium triflate) is used as the ionic salt and 36.6 wt% of PC is used as the plasticizer, one would expect a lower ionic transference number for the Mg^{++} cations (t_{Mg++}) compared to the triflate anions. The presence of PC is expected to enhance the anionic diffusion due to the lowering of viscosity of the polymer gel medium. Table 1 summarizes the ionic conductivity and Mg ion transference number of PEO-based electrolytes compared to the values reported in this study.

Electrochemical characteristics

Cyclic voltammetry of Mg/GPE/Mg symmetrical cells

Electrochemical reversibility of magnesium in PEO:Mgtf-based electrolyte is followed by the symmetrical non-blocking magnesium electrodes [29]. The Mg/GPE/Mg symmetrical cells were subjected to cyclic voltammetry with the scan rate of 5 mV s^{-1}, and voltammogram is shown in Fig. 4. The cathodic and anodic current peaks are clearly observed for the Mg/GPE/Mg symmetrical cell. Higher magnitude

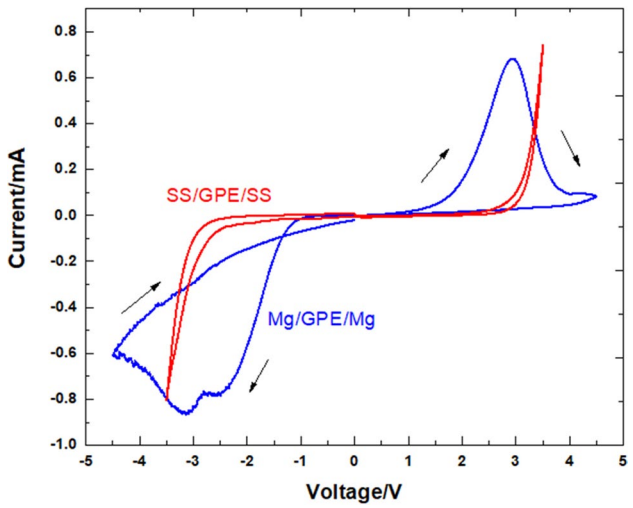

Fig. 4 Cyclic voltammograms of Mg/GPE/Mg and SS/GPE/SS symmetrical cells taken at a scan rate of 5 mV s^{-1} and at 30 °C

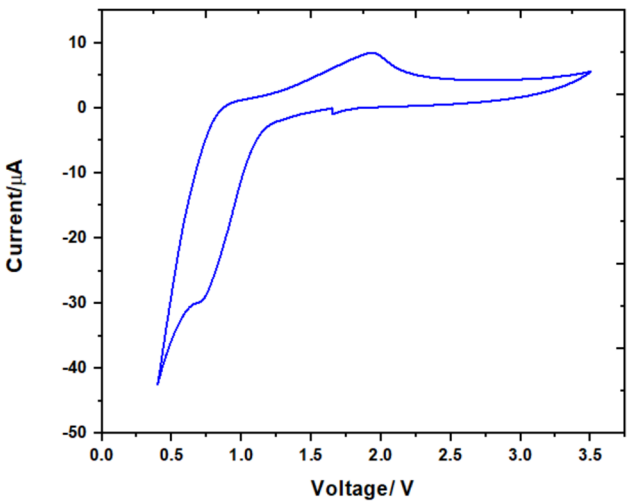

Fig. 5 Cyclic voltammogram at 1 mV s^{-1} scan rate of Mg/GPE/TiO_2-C cell at 30 °C for 0.5–3.0 V voltage window

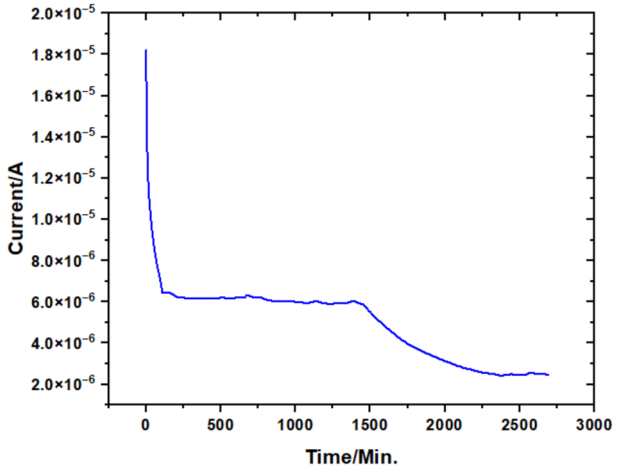

Fig. 6 Constant load discharge characteristics of Mg/PEO:EC:PC: $Mg(CF_3SO_3)_2/TiO_2$-C cell under 60 kΩ load

of cathodic and anodic peak currents of the cell Mg/GPE/Mg suggests that the cathodic deposition and anodic oxidation occur at the Mg/GPE interface according to the reaction given below by Eq. (5) [1]. While the Mg/GPE/Mg system exhibits distinct cathodic and anodic peaks, the cells that have SS-electrodes within the same potential range do not exhibit this feature [40]. This implies that Mg^{++} ion conduction in the polymer electrolyte layer is shown by the easy Mg cathodic deposition and anodic oxidation at the Mg-electrode and polymer electrolyte contact [27, 35].

$$Mg^{+2} + 2e^{-} \leftrightarrow Mg \tag{5}$$

The oxidation of Mg to Mg^{2+} ions takes place during the discharge and the reverse process of electrodeposition of Mg takes place during charging. The voltammograms show the redox peaks corresponding to the deposition (−2.4 V) and dissolution of (2.9 V) of magnesium. Relatively high difference between anodic and cathodic peak potential value is due to the absence of a reference electrode in the system. Similar potential difference (~5 V) between Mg oxidation and reduction has been reported [27]. It also shows that the charges associated with the deposition and dissolution process are equal for the first cycle. This implies that, at the beginning the reversibility of the magnesium deposition and dissolution is high. Electrolyte sample may have traces of moisture, and the additional peak seen at 3.2 V may be attributed to the formation of $Mg(OH)_2$. For the SS/GPE/SS configuration (red curve), the oxidation peak above 3 V is indicative of the electrochemical oxidation of the GPE or residual solvent components, since no active metal (like Mg) is present in the cell. This behavior is commonly observed in symmetric cells and serves to identify the electrochemical stability window of the electrolyte.

Cyclic voltammetry of Mg/GPE/TiO_2-C cell

I-V characteristics of the Mg/GPE/TiO_2-C cell were examined in order to demonstrate the application of the GPE in rechargeable Mg battery. This cyclic voltammogram indicates that the TiO_2 electrode undergoes reduction and oxidation process in the GPE medium. Cyclic voltammogram at 1 mV s^{-1} scan rate of a Mg/GPE/TiO_2-C cell at 30 °C for 0.5–3.0 V voltage windows is shown in Fig. 5. In this potential window, a reduction peak present at 0.75 V is characterized by the insertion of Mg^{++} in to TiO_2 and oxidation peak at 2.0 V is characterized by extraction of Mg^{++} from the cathode. During the charging/discharging process, the main redox reaction of this electrochemical system is Ti^{+4}/Ti^{+3} [24]. A small reduction peak observed in the Fig. 5 at 1.6 V shows that it just starts sweeping from this voltage. From these curves, it possible to calculate the total charge exchanged during the oxidation and reduction process. The calculated values show that the charge associated with the anodic peak (0.015 C) is less than that associated with the cathodic peak (0.026 C). This shows that that the reversibility process at the cathode is poor.

Performance and characterization of the Mg/GPE/TiO_2-C battery

Mg battery was assembled in Mg/GPE/TiO_2-C configuration, and the open circuit voltage was recorded for the

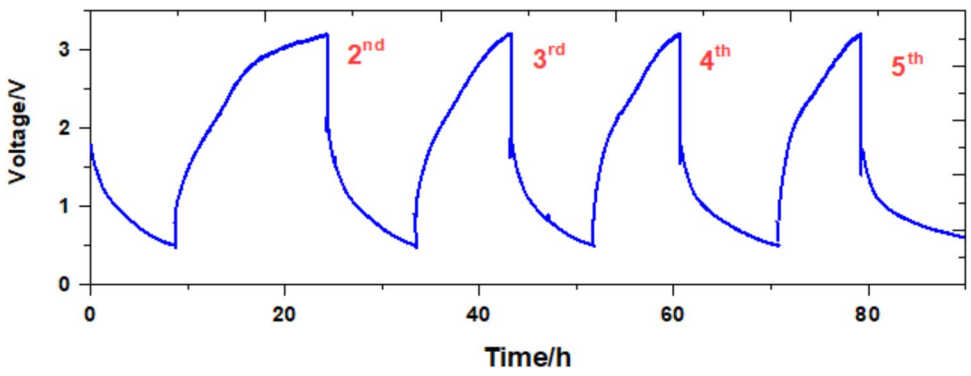

Fig. 7 Charge–discharge curves of a Mg/GPE/TiO_2-C cell at room temperature

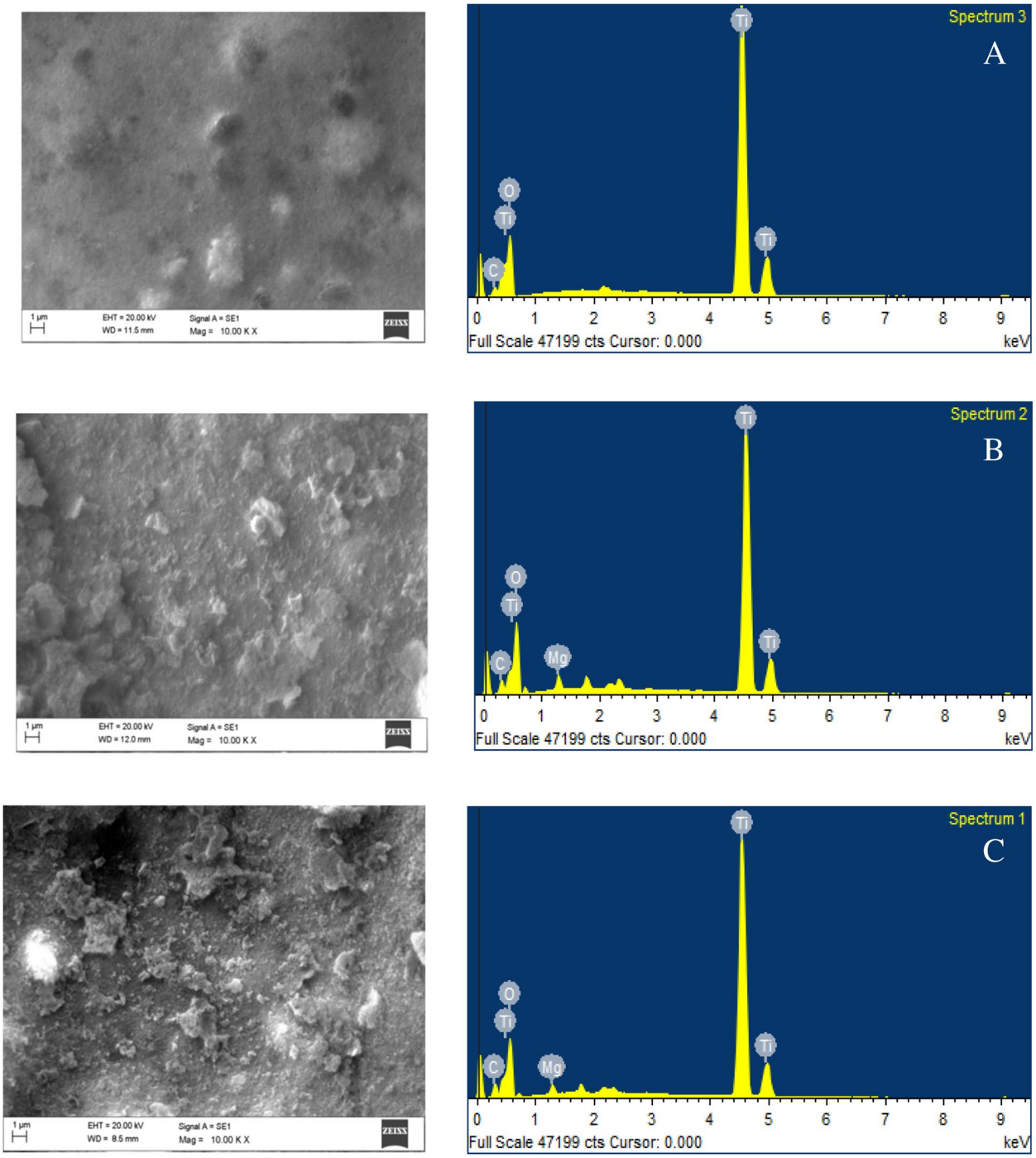

Fig. 8 SEM images and EDAX patterns of **A** as assembled TiO_2-C, **B** TiO_2-C after discharging at 0.015 C rate, **C** TiO_2-C after charging at 0.015 C rate

first 28 h until it became stabilized (not shown). An initial rise in the voltage was observed just after assembling the cell, and after about 5 h, it was stabilized at 1.82 V. This value remained constant up to nearly 28 h until the cell was disconnected. The increase in OCV during the first 2 h can be attributed to the stabilization of the electrode/electrolyte contact.

Figure 6 shows the discharge characteristics of the cell Mg/GPE/TiO_2-C for constant load 60 kΩ. It can be seen that the discharge was sustained for nearly 36 h for the 60

kΩ load. Discharge is characterized by insertion of Mg^{++} ions into TiO_2 structure.

The value of the discharge capacity C was calculated by integrating the area under the curve of Fig. 6 (Eq. 6) as described by the literature [41, 42].

$$C = \frac{\int_0^t I(t)dt}{M} \tag{6}$$

where M is the mass of the active material (TiO_2) in the cathode. Estimated discharge capacity of the Mg/GPE/TiO_2-C cell is 200 mA h g^{-1} for 60 kΩ with an open circuit voltage of 1.85 V which is consistent with previously reported values [43, 44]. The current profile of the first discharge of the battery through the 60 kΩ load exhibits one distinct plateau regions.

Charge/discharge characteristics of the fabricated cells were obtained by using a Metrohm.

Autolab potentiostat/galvanostat (PGSTAT 128 N) system. Charge/discharge rates of 0.015 C (assuming that the theoretical capacity of TiO_2 is 330 mA h g^{-1}) were applied during cell cycling with in the 3.2–0.5 V potential window (Fig. 7).

Charge capacity of TiO_2 lies in the voltage range from 0.75 to 3.2 V, but in the discharge, the most of capacity is released below 2 V. This agrees well with charge discharge cycles shown in Fig. 7. In Fig. 7, a sudden voltage drop from 3.2 V to just below 2.0 V is observed during discharge, a trend also reported by other research groups [43]. During the initial cycles, the voltage drops from the upper voltage limit to the open-circuit voltage. In subsequent cycles, the voltage drop becomes more pronounced, indicating compatibility of the electrolyte with repeated charging and discharging. Therefore, most of the discharge capacity appears to be below 2.0 V as shown in the voltage profile. When the battery is subjected to continuous charge discharge cycles, the first discharge (insertion of Mg^{++} into the TiO_2 structure) yielded a capacity of 65 mA h g^{-1} while the first charge capacity is 95 mA h g^{-1}. Compared to previously reported data, the sudden voltage drop observed in our system is smaller, suggesting that our electrolyte demonstrates superior performance under charge–discharge cycling.

For the first, second and third cycles, calculated coulombic efficiency values increased from 68 to 97% for the 0.5–3.2 V potential window. In the present study, anatase TiO_2 was used as the active material for the cathode, and it was sintered at 450 °C for 45 min so that influence of OH group is minimized. This may be the reason for the lower fading of the discharge capacity after the first cycle.

In the present study, SEM images of the TiO_2–C cathode reveal distinct morphological changes, while energy-dispersive X-ray spectroscopy (EDAX) indicates compositional differences after the first charge–discharge cycle. Figure 8A shows the morphology and EDAX spectrum of the fresh TiO_2–C surface, confirming the presence of titanium and oxygen. Following the initial discharge process (Fig. 8B), the EDAX spectrum reveals the presence of magnesium ions, accompanied by noticeable changes in surface morphology. After the first charging process (Fig. 8C), magnesium is not fully removed from the cathode; only about 40% of the intercalated Mg is extracted. This incomplete removal contributes significantly to capacity fading during the first cycle. However, in subsequent cycles (second and third), a reduction in capacity fading is observed.

Conclusion

A gel polymer electrolyte composed of PEO (12.20 wt%), $(CF_3SO_3)_2Mg$ (14.6 wt%), EC (36.6 wt%), and PC (36.6 wt%) was investigated for its ionic conductivity, magnesium-ion transport number, and electrochemical behavior via cyclic voltammetry. This electrolyte exhibited a room-temperature ionic conductivity of 2.52×10^{-3} S/cm and a transport number of 0.51. The temperature-dependent DC conductivity followed typical Arrhenius behavior. Electrochemical reversibility of the Mg/Mg^{2+} redox couple was evaluated using cyclic voltammetry and impedance spectroscopy, both confirming favorable magnesium deposition and dissolution kinetics. Rechargeable Mg^{2+} batteries were fabricated using cost-effective TiO_2 as the cathode, the PEO-based gel polymer electrolyte as the separator, and magnesium metal as the anode. Preliminary results from Mg/GPE/TiO_2-C cells demonstrated a discharge capacity of 65 mAh g^{-1}. Although the specific capacity is modest, the cells maintained high cycling efficiency across multiple cycles. SEM and EDAX analyses confirmed the intercalation and deintercalation of magnesium ions in the cathode. Further studies are underway involving gel polymer electrolytes blended with ionic liquids to enhance performance.

Author contributions HN.M. Sarangika conducted the experiments, wrote the main manuscript text, and drew the figures. M.A.K.L. Dissanayake and G.K.R. Senadeera provided the lab facilities to conduct the experiments.

Funding Not Applicable.

Data availability Not Applicable.

Declarations

Ethics approval This article does not involve human or biological research and has no moral or ethical issues.

Competing interests The authors declare no competing interests.

References

1. Tarascon J-M, Armand M (2001) Issues and challenges facing rechargeable lithium batteries. Nature 414:359–367. https://doi.org/10.1038/35104644
2. Kumar GG, Munichandraiah N (1999) Reversibility of Mg/Mg2+ couple in a gel polymer electrolyte. Electrochim Acta 44:2663–2666. https://doi.org/10.1016/S0013-4686(98)00388-0
3. Wang H, Yao C-J, Nie H-J et al (2020) Recent progress in carbonyl-based organic polymers as promising electrode materials for lithium-ion batteries (LIBs). J Mater Chem A 8:11906–11922. https://doi.org/10.1039/D0TA03321A
4. Sun T, Xie J, Guo W et al (2020) Covalent–organic frameworks: advanced organic electrode materials for rechargeable batteries. Adv Energy Mater 10:1904199. https://doi.org/10.1002/aenm.201904199
5. Zhang W, Liu Y, Guo Z (2019) Approaching high-performance potassium-ion batteries via advanced design strategies and engineering. Sci Adv 5:eaav7412. https://doi.org/10.1126/sciadv.aav7412
6. Pan H, Hu Y-S, Chen L (2013) Room-temperature stationary sodium-ion batteries for large-scale electric energy storage. Energy Environ Sci 6:2338. https://doi.org/10.1039/c3ee40847g
7. Zhao X, Xiong P, Meng J et al (2017) High rate and long cycle life porous carbon nanofiber paper anodes for potassium-ion batteries. J Mater Chem A 5:19237–19244. https://doi.org/10.1039/C7TA04264G
8. Zhang R, Yu X, Nam K-W et al (2012) α-MnO2 as a cathode material for rechargeable Mg batteries. Electrochem Commun 23:110–113. https://doi.org/10.1016/j.elecom.2012.07.021
9. Sheha E, El-Deftar M (2018) Magnesium hexakis(methanol)-dinitrate complex electrolyte for use in rechargeable magnesium batteries. J Solid State Electrochem 22:2671–2679. https://doi.org/10.1007/s10008-018-3986-z
10. Luo L, Zhen Y, Lu Y et al (2020) Structural evolution from layered Na 2 Ti 3 O 7 to Na 2 Ti 6 O 13 nanowires enabling a highly reversible anode for Mg-ion batteries. Nanoscale 12:230–238. https://doi.org/10.1039/C9NR08003A
11. Bella F, De Luca S, Fagiolari L et al (2021) An overview on anodes for magnesium batteries: challenges towards a promising storage solution for renewables. Nanomaterials 11:810. https://doi.org/10.3390/nano11030810
12. Aurbach D, Lu Z, Schechter A et al (2000) Prototype systems for rechargeable magnesium batteries. Nature 407:724–727. https://doi.org/10.1038/35037553
13. Bucur CB, Gregory T, Oliver AG, Muldoon J (2015) Confession of a magnesium battery. J Phys Chem Lett 6:3578–3591. https://doi.org/10.1021/acs.jpclett.5b01219
14. Arthur TS, Zhang R, Ling C et al (2014) Understanding the electrochemical mechanism of K-αMnO 2 for magnesium battery cathodes. ACS Appl Mater Interfaces 6:7004–7008. https://doi.org/10.1021/am5015327
15. Yin J, Pelliccione CJ, Lee SH et al (2016) Communication—sol-gel synthesized magnesium vanadium oxide, Mg x V 2 O 5 · nH 2 O: the role of structural Mg 2+ on battery performance. J Electrochem Soc 163:A1941–A1943. https://doi.org/10.1149/2.0781609jes
16. Liu M, Jain A, Rong Z et al (2016) Evaluation of sulfur spinel compounds for multivalent battery cathode applications. Energy Environ Sci 9:3201–3209. https://doi.org/10.1039/C6EE01731B
17. Sun X, Bonnick P, Duffort V et al (2016) A high capacity thiospinel cathode for Mg batteries. Energy Environ Sci 9:2273–2277. https://doi.org/10.1039/C6EE00724D
18. Saha P, Jampani PH, Datta MK et al (2017) A rapid solid-state synthesis of electrochemically active Chevrel phases (Mo6T8; T = S, Se) for rechargeable magnesium batteries. Nano Res 10:4415–4435. https://doi.org/10.1007/s12274-017-1695-z
19. Liu B, Luo T, Mu G et al (2013) Rechargeable Mg-ion batteries based on WSe 2 nanowire cathodes. ACS Nano 7:8051–8058. https://doi.org/10.1021/nn4032454
20. Novák P, Imhof R, Haas O (1999) Magnesium insertion electrodes for rechargeable nonaqueous batteries — a competitive alternative to lithium? Electrochim Acta 45:351–367. https://doi.org/10.1016/S0013-4686(99)00216-9
21. Madej E, La Mantia F, Mei B et al (2014) Reliable benchmark material for anatase TiO2 in Li-ion batteries: on the role of dehydration of commercial TiO2. J Power Sources 266:155–161. https://doi.org/10.1016/j.jpowsour.2014.05.018
22. Yuan X, Xu Q, Liu X et al (2016) Layered cathode material with improved cycle performance and capacity by surface anchoring of TiO 2 nanoparticles for Li-ion batteries. Electrochim Acta 213:648–654. https://doi.org/10.1016/j.electacta.2016.07.157
23. Le TS, Hoa TH, Truong DQ (2019) Shape-controlled F-doped TiO2 nanocrystals for Mg-ion batteries. J Electroanal Chem 848:113293. https://doi.org/10.1016/j.jelechem.2019.113293
24. Su S, Huang Z, NuLi Y et al (2015) A novel rechargeable battery with a magnesium anode, a titanium dioxide cathode, and a magnesium borohydride/tetraglyme electrolyte. Chem Commun 51:2641–2644. https://doi.org/10.1039/C4CC08774G
25. Deivanayagam R, Ingram BJ, Shahbazian-Yassar R (2019) Progress in development of electrolytes for magnesium batteries. Energy Storage Mater 21:136–153. https://doi.org/10.1016/j.ensm.2019.05.028
26. Jathushan V, Jayamaha JHTB, Wijayasinghe HWMAC, Vignarooban K (2022) Electrochemical studies on poly(ethylene oxide) based gel-polymer electrolytes for magnesium-ion batteries. Mater Sci Forum 1077:229–234. https://doi.org/10.4028/p-8k8x71
27. Kumar Y, Hashmi SA, Pandey GP (2011) Ionic liquid mediated magnesium ion conduction in poly(ethylene oxide) based polymer electrolyte. Electrochim Acta 56:3864–3873. https://doi.org/10.1016/j.electacta.2011.02.035
28. Sharma J, Hashmi SA (2013) Magnesium ion transport in poly(ethylene oxide)-based polymer electrolyte containing plastic-crystalline succinonitrile. J Solid State Electrochem 17:2283–2291. https://doi.org/10.1007/s10008-013-2104-5
29. Sarangika HNM, Dissanayake MAKL, Senadeera GKR et al (2017) Polyethylene oxide and ionic liquid-based solid polymer electrolyte for rechargeable magnesium batteries. Ionics (Kiel) 23:2829–2835. https://doi.org/10.1007/s11581-016-1870-3
30. Sarangika HNM, Shashintha HTG, Dissanayake MAKL, Senadeera GKR (2024) Effect of TiO2 nano fillers on ionic conductivity enhancement in Mg(BH4)2:polyethylene oxide (PEO) polymer gel electrolyte. J Solid State Electrochem 28:2163–2173. https://doi.org/10.1007/s10008-023-05748-8
31. Maheshwaran C, Mishra K, Kanchan DK, Kumar D (2020) Mg 2 + conducting polymer gel electrolytes : physical and electrochemical investigations. https://doi.org/10.1007/s11581-020-03459-y
32. Maheshwaran C, Kanchan DK, Gohel K et al (2020) Effect of Mg (CF 3 SO 3) 2 concentration on structural and electrochemical properties of ionic liquid incorporated polymer electrolyte membranes. J Solid State Electrochem 24:655–665
33. Sheha E (2013) Prototype system for magnesium/TiO2 anatase batteries. Int J Electrochem Sci 8:3653–3663. https://doi.org/10.1016/S1452-3981(23)14420-8
34. Banitaba SN, Semnani D, Heydari-Soureshjani E et al (2020) The effect of concentration and ratio of ethylene carbonate and propylene carbonate plasticizers on characteristics of the electrospun PEO-based electrolytes applicable in lithium-ion batteries. Solid State Ionics 347:115252. https://doi.org/10.1016/j.ssi.2020.115252

35. Girish Kumar G, Munichandraiah N (2000) Effect of plasticizers on magnesium-poly(ethyleneoxide) polymer electrolyte. J Electroanal Chem 495:42–50. https://doi.org/10.1016/S0022-0728(00)00404-6
36. Dissanayake MAKL, Rupasinghe WNS, Seneviratne VA et al (2014) Optimization of iodide ion conductivity and nano filler effect for efficiency enhancement in polyethylene oxide (PEO) based dye sensitized solar cells. Electrochim Acta 145:319–326. https://doi.org/10.1016/j.electacta.2014.09.017
37. Anilkumar KM, Jinisha B, Manoj M, Jayalekshmi S (2017) Poly(ethylene oxide) (PEO) – Poly(vinyl pyrrolidone) (PVP) blend polymer based solid electrolyte membranes for developing solid state magnesium ion cells. Eur Polym J 89:249–262. https://doi.org/10.1016/j.eurpolymj.2017.02.004
38. Yoshimoto N, Yakushiji S, Ishikawa M, Morita M (2003) Rechargeable magnesium batteries with polymeric gel electrolytes containing magnesium salts. Electrochim Acta 48:2317–2322. https://doi.org/10.1016/S0013-4686(03)00221-4
39. Morita M, Shirai T, Yoshimoto N, Ishikawa M (2005) Ionic conductance behavior of polymeric gel electrolyte containing ionic liquid mixed with magnesium salt. J Power Sources 139:351–355. https://doi.org/10.1016/j.jpowsour.2004.07.028
40. Maheshwaran C, Kanchan DK, Mishra K et al (2020) Flexible magnesium-ion conducting polymer electrolyte membranes: mechanical, structural, thermal, and electrochemical impedance spectroscopic properties. J Mater Sci Mater Electron 31:15013–15027. https://doi.org/10.1007/s10854-020-04065-4
41. Sheha E, El-Mansy MK (2008) A high voltage magnesium battery based on H2SO4-doped (PVA)0.7(NaBr)0.3 solid polymer electrolyte. J Power Sources 185:1509–1513. https://doi.org/10.1016/j.jpowsour.2008.09.046
42. Sheha E (2009) Ionic conductivity and dielectric properties of plasticized PVA0.7(LiBr)0.3(H2SO4)2.7M solid acid membrane and its performance in a magnesium battery. Solid State Ionics 180:1575–1579. https://doi.org/10.1016/j.ssi.2009.10.008
43. Narayanan NSV, Raj BVA, Sampath S (2009) Electrochemistry communications magnesium ion conducting, room temperature molten electrolytes. Electrochem commun 11:2027–2031. https://doi.org/10.1016/j.elecom.2009.08.045
44. Pandey GP, Agrawal RC, Hashmi SA (2011) Magnesium ion-conducting gel polymer electrolytes dispersed with fumed silica for rechargeable magnesium battery application. 2253–2264. https://doi.org/10.1007/s10008-010-1240-4